DOI: 10.1002/adma.200501756

Low-Temperature Synthesis of Star-Shaped PbS Nanocrystals in Aqueous Solutions of Mixed Cationic/Anionic Surfactants**

By *Nana Zhao* and *Limin Qi**

Obtaining control over the morphology of colloidal nanocrystals with well-defined shapes remains an important goal of modern materials chemistry, since shape-controlled nanocrystals are promising candidates as active components in a wide range of technological applications, and are model systems for the study of nanoscale shape-dependent properties.[1] In particular, the shape-controlled synthesis of colloidal nanocrystals of metal chalcogenide semiconductors, such as cadmium chalcogenides,[1a,b,2] lead chalcogenides,[3] Ag_2S,[4] and MnS,[3b,5] has attracted intensive interest; in this regard, synthetic methods based on high-temperature (typically 120–360 °C) reactions in organic solutions involving capping agents have most often been employed. Although this high-temperature organic solution approach has been demonstrated to be a promising method for achieving morphological control of semiconductor nanocrystals, low-temperature synthesis in aqueous solutions is highly desirable because it represents an environmentally benign and user-friendly approach, which may be considered to be a relatively green chemical alternative of practical significance.[6] However, the development of a facile, low-temperature synthesis of shape-controlled semiconductor nanocrystals in aqueous solutions remains a great challenge. It is to be noted that mixtures of various surfactants, including alkyl amines, alkyl acids, alkylphosphonic acids, and trioctyl phosphine oxide (TOPO), are frequently used as capping agents to tailor the crystal shape in high-temperature solution-phase syntheses. Recently, we have demonstrated that the low-temperature synthesis of morphology-controlled one-dimensional (1D) $BaXO_4$ (where X = Cr, Mo, W) nanostructures and their hierarchical architectures can be readily achieved in reverse-micelle solutions of mixed cationic/anionic surfactants.[7] These results have inspired us to explore the low-temperature synthesis of semiconductor nanocrystals with tailored shapes in aqueous solutions of mixed cationic/anionic surfactants.

[*] Prof. L. Qi, N. Zhao
State Key Laboratory for Structural Chemistry of Unstable and Stable Species
College of Chemistry, Peking University
Beijing 100871 (P.R. China)
E-mail: liminqi@pku.edu.cn

[**] Support from NSFC (20325312, 20473003, 20233010) and FANEDD (200020) is gratefully acknowledged. Supporting Information is available online from Wiley InterScience or from the author.

As a π–π semiconductor with a narrow bandgap (0.41 eV) and a large exciton Bohr radius (18 nm), PbS shows extensive quantum-size effects in nanocrystalline form and has wide-ranging potential applications, such as in near-IR (NIR) communication, optical switches, thermal and biological imaging, photovoltaics, and solar cells.[3a,8] While much effort has been devoted to the size-controlled synthesis of PbS quantum dots with tunable optical properties,[9] there are only a few reports on the shape-controlled synthesis of high-quality colloidal PbS nanocrystals.[3a,b] Notably, PbS nanocrystals with a variety of novel shapes, including rod-based multipods, truncated octahedrons, cubes, and stars with six symmetric horns, were successfully produced by the thermal decomposition of a molecular precursor in hot phenyl ether solvent at temperatures varying from 140 to 250 °C.[3a] The obtained star-shaped PbS nanocrystals (50–60 nm in size) represent novel nanoscale structures, but their optical properties have not been reported. Herein, we report a facile synthesis of uniform star-shaped PbS nanocrystals (40–100 nm in size), as well as octahedral PbS nanocrystals, in aqueous solutions of mixed cationic/anionic surfactants at a low temperature of 80 °C.

The synthesis of star-shaped PbS nanocrystals has been achieved by the thermal decomposition of thioacetamide (TAA) in aqueous solutions of lead acetate in the presence of the cationic surfactant cetyltrimethylammonium bromide (CTAB) and the anionic surfactant sodium dodecyl sulfate (SDS). Figure 1a shows a low-magnification scanning electron microscopy (SEM) image of the PbS product obtained after a reaction time of 5 h, indicating the exclusive formation of uniform star-like nanocrystals. The related X-ray diffraction (XRD) pattern (Fig. S1, Supporting Information) shows sharp peaks corresponding to cubic PbS with a rock salt structure (Joint Committee on Powder Diffraction Standards (JCPDS) No. 5-592), confirming the formation of pure PbS nanocrystals. An enlarged SEM image shown in Figure 1b suggests that the stars exhibit a well-defined star-shaped geometry with six symmetrical horns, and the crystal size determined from the distance between two neighboring vertices is ~90 nm. The corresponding transmission electron microscopy (TEM) image (Fig. 1c) clearly shows a two-dimensional (2D) projection of the three-dimensional (3D) six-horn stars, indicating a regular deposition of most stars on the copper grid with three horns stably standing on the substrate. The crystal size determined from the distance between two alternating tips is ~90 nm, in good agreement with the crystal size measured from the SEM image. The electron diffraction (ED) pattern

ADVANCED MATERIALS

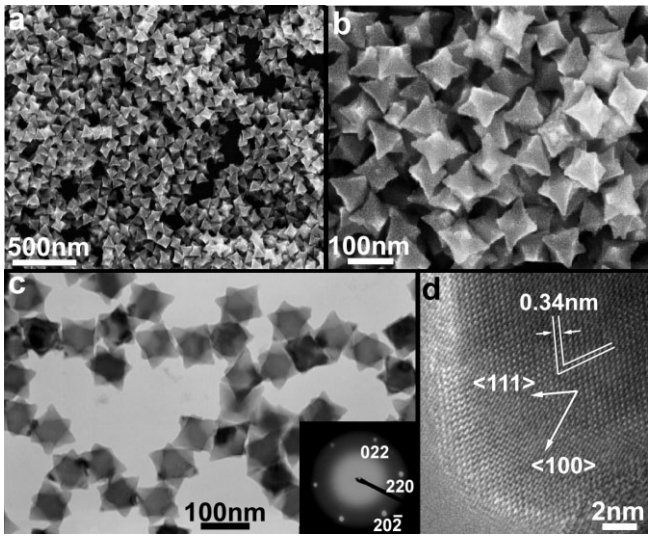

Figure 1. a,b) SEM, c) transmission electron microscopy (TEM), and d) high-resolution TEM images of star-shaped PbS nanocrystals obtained in mixed CTAB/SDS solution after a reaction time of 5 h. The inset in (c) shows the electron diffraction (ED) pattern obtained from an individual PbS star.

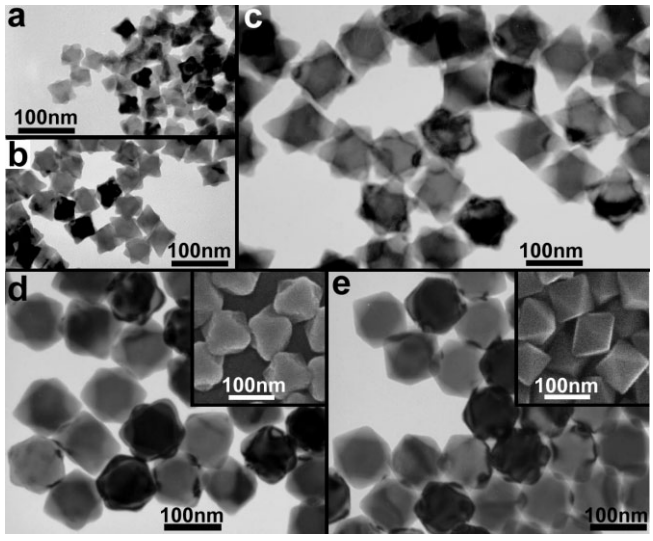

Figure 2. TEM images of PbS nanocrystals obtained in mixed CTAB/SDS solution after reaction times of: a) 1 h, b) 2 h, c) 12 h, d) 1 day, and e) 2 days. Insets in (d,e) show the corresponding SEM images.

from a single star shows diffraction spots due to the [111] zone axis of cubic PbS, indicating that the six-horn star is actually a PbS single crystal with the six horns grown along the <100> direction. The single crystallinity of the stars is further confirmed by the high-resolution TEM (HRTEM) image shown in Figure 1d, which has been obtained from a [110]-projected star that serendipitously had two horns standing on the substrate, showing the <100> direction of each horn. These single-crystalline, six-horn PbS nanostars are reminiscent of the well-defined but rather rounded star-shaped PbS nanocrystals obtained by Cheon and co-workers through the high-temperature (230 °C) solution-phase approach.[3a]

It has been found that the size of the star-shaped PbS nanocrystals can be nicely controlled by adjusting the reaction time. Also, the star-shaped morphology evolves into a regular octahedron after a prolonged reaction time. Figure 2 shows micrographs of the PbS products harvested at different intervals of the reaction. Star-shaped nanocrystals obtained at shorter reaction times of 1 h and 2 h have sizes of ~42 nm and 50 nm, respectively (Figs. 2a,b); after 5 h of reaction (Fig. 1), the stars grow to be ~90 nm. With increasing reaction time from 5 h to 12 h, the size of the star-shaped nanocrystals further grows to ~100 nm with their well-defined star-shaped morphology still unchanged (Fig. 2c). However, if the reaction time is further increased to 1 day, the crystal size remains unchanged (~100 nm), but the morphology evolves towards octahedrons with the depressed portion of the stars being partially filled (Fig. 2d). After a reaction time of 2 days, the depressed portion of the stars is completely filled, resulting in the formation of regular PbS octahedrons, ~100 nm in size (Fig. 2e). Since the crystal size (i.e., the distance between two neighboring vertices) remains unchanged during the transformation from stars to octahedrons, it is possible to conclude that the transformation occurs via the addition of PbS species that are newly produced by the slow, continued reaction rather than via intraparticle Ostwald ripening or surface diffusion. In addition, the size of the star-shaped PbS nanocrystals can also be adjusted by changing the reactant concentration; for example, monodisperse, well-defined PbS nanostars, ~72 nm in size, are fabricated at a lower reactant concentration (Fig. S2, Supporting Information).

Since the obtained star-shaped and octahedral PbS nanocrystals (40–100 nm) are considerably larger than the exciton Bohr radius (18 nm), quantum-confinement effects are not expected. However, quantum confinement can possibly occur near the tip edge of the stars, which are smaller than or comparable to the PbS Bohr radius, since the optical properties of non-spherical nanocrystals are controlled by the lowest dimension of the nanocrystal.[10] For star-shaped semiconductor nanocrystals with thin tips exhibiting quantum confinement, it can be envisioned that the bandgap energy increases from the inner thicker part to the tip edge of the crystals due to position-dependent quantum-size effects.[11] Therefore, the absorption spectra of the obtained PbS nanocrystals with well-defined shapes has been measured in order to reveal any possible shape-dependent optical properties. Figure 3 shows the absorption spectra of the PbS nanocrystals obtained at three different reaction times after redispersion in water. The smaller PbS nanostars (~42 nm) obtained after a reaction time of 1 h show a clear excitonic absorption peak at ~324 nm; the larger PbS nanostars (~100 nm) obtained after 12 h show an absorption peak at ~500 nm and two absorption shoulders around 330 and 680 nm; and the regular PbS nanooctahedrons (~100 nm) obtained after 2 days show two excitonic peaks at ~344 and 485 nm. While our experiments indi-

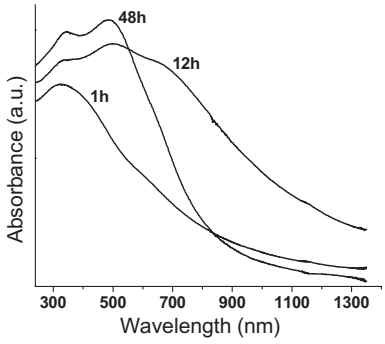

Figure 3. Absorption spectra of PbS nanocrystals obtained in mixed CTAB/SDS solution after different reaction times.

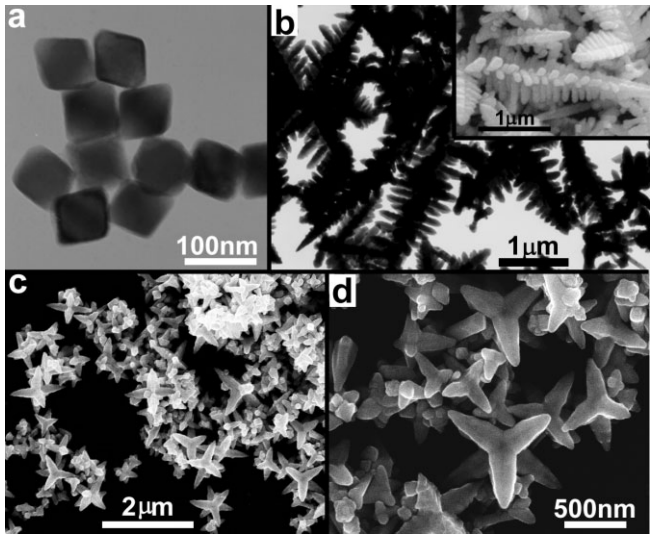

Figure 4. a,b) TEM and c,d) SEM images of PbS crystals obtained in single CTAB (a) and SDS solution (b–d): a) [CTAB] = 5.7 mM, 5 h; b) [SDS] = 1.1 mM, 5 h; c,d) [SDS] = 11 mM, 14 h. The inset in (b) shows the corresponding SEM image.

cate that the measurements are highly reproducible, this result is quite surprising since it indicates a remarkable blue-shift from the absorption onset of bulk PbS (~3020 nm) for PbS nanocrystals with overall sizes much larger than the Bohr radius. An exact assignment of the absorption peaks is not possible at the present time; however, it can be reasonably speculated that position-dependent quantum-size effects exist for the relatively large but highly faceted nanocrystals (stars and octahedrons) with regular shapes and thin tips, resulting in several dramatically blue-shifted excitonic absorptions. In this context, the large Bohr radius of PbS (18 nm) largely contributes to the observation of shape-dependent optical properties for PbS semiconductor nanocrystals, considering that these optical properties are rarely observed for other semiconductors with smaller Bohr radius values. However, there is another possibility that the observed peaks may correspond to transitions into high-energy bands rather than excitonic transitions. Moreover, scattering effects also need be taken into account since the particles are comparable in size to the wavelength of light in the present case. Indeed, the origin of the observed absorption peaks in the UV-visible region is still far from well understood, and more detailed investigations are needed to elucidate the interesting shape-dependent optical properties of the star-shaped PbS nanocrystals.

The presence of the CTAB/SDS mixture in the system plays a key role in the formation of star-shaped PbS nanocrystals. Large star-shaped PbS crystals with eight <111>-oriented arms are produced in the absence of surfactants under otherwise similar conditions.[12] After a reaction time of 5 h, PbS octahedrons (~70 nm in size) are obtained in the presence of 5.7 mM CTAB (Fig. 4a), whereas dendritic PbS crystals partly preserving the hierarchical structure of the original eight-arm stars are produced in the presence of 1.1 mM SDS (Fig. 4b). If a higher SDS concentration (11 mM) is employed, submicrometer-sized stars with six symmetry arms as well as some irregular crystals are obtained after 14 h of reaction (Figs. 4c,d). These results indicate that the presence of SDS considerably accelerates the growth of the {100} faces relative to the {111} faces, leading to the formation of hexapods with six <100>-oriented arms, whereas the presence of CTAB tends to just bring about a mild increase in the growth rate of the {100} faces relative to the {111} faces, which favors the formation of octahedrons with eight {111} faces. It is known that the intrinsic surface energy of the {111} faces of cubic PbS, containing Pb or S only, is higher than that of the {100} faces, which contain mixed Pb/S.[1g] Capping molecules like SDS and CTAB selectively stabilize the {111} faces since their ionic headgroups can strongly interact with the charged {111} faces rather than the uncharged {100} faces. Considering that the interaction between Pb and $-SO_4^-$ ions may be larger than that between S and $-N(CH_3)_3^+$ ions, a larger decrease in the surface energy of the {111} faces is expected for SDS, leading to relatively greater accelerated growth on the {100} faces relative to the {111} faces. As a result, the presence of the binary CTAB/SDS mixture results in the formation of star-shaped PbS nanocrystals as an intermediate morphology between hexapods with six <100>-oriented arms and octahedrons with eight {111} faces due to a cooperative effect of CTAB and SDS. Considering that it is difficult to control the size of the PbS hexapods within 100 nm in single SDS systems, it is likely that size and morphology control of the PbS nanocrystals is established by cooperative effects of the binary surfactants. Hence, the mixed CTAB/SDS surfactants may play the role of binary capping agents in the nucleation and growth of PbS crystals, leading to the gradual growth of star-shaped PbS nanocrystals during the early reaction stages (up to 12 h) when there is a high monomer concentration, which is favorable for anisotropic crystal growth.[13] However, after 12 h of reaction, anisotropic growth along the <100>-oriented horns of the PbS stars is restricted, and a more stable form (i.e., the octahedron) is preferred as the monomer concentration decreases to approach a thermodynamic growth regime.[13]

It is found that a mixing ratio of CTAB to SDS in the range of 4–6:1 is favorable for the formation of star-shaped nano-

ADVANCED MATERIALS

crystals, and a mixing ratio of ~1:1 usually results in irregular plate-like crystals. We tentatively suggest that mixed CTAB/SDS micelles in the reaction solution at 80 °C may directly participate in the shape-controlled synthesis of PbS nanostars, since mixed micelles are generally the predominant structures in clear solutions of CTAB/SDS mixtures at mixing ratios far away from 1:1.[14] It has been documented that in mixed CTAB/SDS solutions, relatively larger catanionic vesicles and surfactant salts rather than mixed micelles tend to form at the equimolar mixing ratio (CTAB/SDS = 1:1).[15] Therefore, in the equimolar CTAB/SDS solution, a wide variety of microstructures possibly coexist, especially at the early stage of the reaction when the solution is heated to 80 °C. Consequently, irregularly shaped nuclei are formed, possibly due to the influence of the various microstructures, resulting in the final formation of irregular plate-like PbS crystals. Therefore, the formation of homogeneous mixed micelles is an essential condition for the controlled growth of uniform star-shaped PbS nanocrystals. In addition, such a synthetic method based on aqueous solutions of mixed cationic/anionic surfactants can be readily extended to the synthesis of PbS nanocrystals with other morphologies. For example, unique single-crystalline PbS nanobelts (~20 nm in thickness) grown along the [110] direction can be fabricated in the presence of didodecyldimethylammonium bromide (DDAB)/SDS mixtures with a suitable mixing ratio under otherwise similar synthesis conditions (Fig. S3, Supporting Information). However, the exact mechanism for the morphological control of PbS nanocrystals by mixed cationic/anionic surfactants is worthy of further investigation.

In summary, a facile, water-based, low-temperature synthesis of well-defined, star-shaped PbS nanocrystals with tunable sizes (40–100 nm) has been demonstrated. This result provides a useful model system for investigating the shape-dependent optical properties of semiconductor nanocrystals, and may open new avenues for the green chemical synthesis of shape-controlled nanocrystals.

Experimental

The synthetic procedure previously reported for fabricating micrometer-sized, star-shaped PbS crystals with eight symmetric arms, involving the thermal decomposition of TAA in aqueous solutions of lead acetate and acetic acid [12], was modified for the current synthesis of star-shaped PbS nanocrystals by adding the cationic surfactant CTAB and the anionic surfactant SDS. In a typical synthesis, 3.0 mL of water, 0.5 mL of 0.05 M CTAB, 0.1 mL of 0.05 M SDS, and 0.4 mL of 1 M acetic acid were mixed at room temperature, followed by the addition of 0.2 mL of 0.5 M $Pb(OAc)_2$ and 0.2 mL of 0.5 M TAA under stirring, giving concentrations of 5.7 mM and 1.1 mM for CTAB and SDS, respectively. The resultant translucent solution was thermostated at 80 °C for a certain time under static conditions, resulting in a brown colloid solution. The colloidal particles were collected by centrifugation, washed with water, and dried in air. The obtained products were characterized by SEM (FEI Strata DB235), TEM (JEOL JEM-200CX), HRTEM (FEI Tecnai F30), XRD (Rigaku Dmax-2000 with Cu Kα radiation), and UV-vis-NIR spectroscopy (Shimadzu UV-3100).

Received: August 22, 2005
Final version: November 10, 2005
Published online: January 10, 2006

[1] a) X. Peng, L. Manna, W. Yang, J. Wickham, E. Scher, A. Kadavanich, A. P. Alivisatos, *Nature* **2000**, *404*, 59. b) L. Manna, D. J. Milliron, A. Meidel, E. C. Scher, A. P. Alivisatos, *Nat. Mater.* **2003**, *2*, 382. c) R. Jin, Y. Cao, C. A. Mirkin, K. L. Kelly, G. C. Schatz, J. G. Zheng, *Science* **2001**, *294*, 1901. d) Y. Sun, Y. Xia, *Science* **2002**, *298*, 2176. e) H. Cölfen, S. Mann, *Angew. Chem. Int. Ed.* **2003**, *42*, 2350. f) C. Burda, X. Chen, R. Narayanan, M. A. El-Sayed, *Chem. Rev.* **2005**, *105*, 1025. g) Y.-W. Jun, J.-H. Lee, J.-S. Choi, J. Cheon, *J. Phys. Chem. B* **2005**, *109*, 14795.

[2] a) L. Manna, E. C. Scher, A. P. Alivisatos, *J. Am. Chem. Soc.* **2000**, *122*, 12700. b) Z. A. Peng, X. Peng, *J. Am. Chem. Soc.* **2001**, *123*, 183. c) Z. A. Peng, X. Peng, *J. Am. Chem. Soc.* **2002**, *124*, 3343. d) X. Peng, *Adv. Mater.* **2003**, *15*, 459. e) Y.-W. Jun, S.-M. Lee, N.-J. Kang, J. Cheon, *J. Am. Chem. Soc.* **2001**, *123*, 5150.

[3] a) S.-M. Lee, Y.-W. Jun, S.-N. Cho, J. Cheon, *J. Am. Chem. Soc.* **2002**, *124*, 11244. b) J. Joo, H. B. Na, T. Yu, J. H. Yu, Y. W. Kim, F. Wu, J. Z. Zhang, T. Hyeon, *J. Am. Chem. Soc.* **2003**, *125*, 11100. c) W. Lu, J. Fang, K. L. Stokes, J. Lin, *J. Am. Chem. Soc.* **2004**, *126*, 11798. d) J. M. Pietryga, R. D. Schaller, D. Werder, M. H. Stewart, V. I. Klimov, J. A. Hollingsworth, *J. Am. Chem. Soc.* **2004**, *126*, 11752. e) K.-S. Cho, D. V. Talapin, W. Gaschler, C. B. Murray, *J. Am. Chem. Soc.* **2005**, *127*, 7140.

[4] W. P. Lim, Z. Zhang, H. Y. Low, W. S. Chin, *Angew. Chem. Int. Ed.* **2004**, *43*, 5685.

[5] Y.-W. Jun, Y.-Y. Jung, J. Cheon, *J. Am. Chem. Soc.* **2002**, *124*, 615.

[6] X. Peng, *Chem. Eur. J.* **2002**, *8*, 335.

[7] a) H. Shi, L. Qi, J. Ma, H. Cheng, *J. Am. Chem. Soc.* **2003**, *125*, 3450. b) H. Shi, L. Qi, J. Ma, H. Cheng, B. Zhu, *Adv. Mater.* **2003**, *15*, 1647. c) H. Shi, L. Qi, J. Ma, N. Wu, *Adv. Funct. Mater.* **2005**, *15*, 442.

[8] a) S. A. McDonald, G. Konstantatos, S. Zhang, P. W. Cyr, E. J. D. Klem, L. Levina, E. H. Sargent, *Nat. Mater.* **2005**, *4*, 138. b) L. Levina, V. Sukhovatkin, S. Musikhin, S. Cauchi, R. Nisman, D. P. Bazett-Jones, E. H. Sargent, *Adv. Mater.* **2005**, *17*, 1854. c) K. R. Choudhury, Y. Sahoo, S. Jang, P. N. Prasad, *Adv. Funct. Mater.* **2005**, *15*, 751. d) J.-P. Ge, J. Wang, H.-X. Zhang, X. Wang, Q. Peng, Y.-D. Li, *Chem. Eur. J.* **2005**, *11*, 1889. e) D. Kuang, A. Xu, Y. Fang, H. Liu, C. Frommen, D. Fenske, *Adv. Mater.* **2003**, *15*, 1747.

[9] a) M. A. Hines, G. D. Scholes, *Adv. Mater.* **2003**, *15*, 1844. b) L. Bakueva, I. Gorelikov, S. Musikhin, X. S. Zhao, E. H. Sargent, E. Kumacheva, *Adv. Mater.* **2004**, *16*, 926. c) S. Wu, H. Zeng, Z. A. Schelly, *Langmuir* **2005**, *21*, 686.

[10] K. K. Nanda, S. N. Dahu, *Adv. Mater.* **2001**, *13*, 280.

[11] W.-S. Chae, H.-W. Shin, E.-S. Lee, E.-J. Shin, J.-S. Jung, Y.-R. Kim, *J. Phys. Chem. B* **2005**, *109*, 6204.

[12] Y. Ma, L. Qi, J. Ma, H. Cheng, *Cryst. Growth Des.* **2004**, *4*, 351.

[13] S.-M. Lee, S.-N. Cho, J. Cheon, *Adv. Mater.* **2003**, *15*, 441.

[14] H. Chakraborty, M. Sarkar, *Langmuir* **2004**, *20*, 3551.

[15] V. Tomašic, I. Štefanic, N. Filipovic-Vincekovic, *Colloid Polym. Sci.* **1999**, *277*, 153.

